Double- β Decay

OMITTED FROM SUMMARY TABLE NEUTRINOLESS DOUBLE- β DECAY

Revised August 2019 by A. Piepke (University of Alabama) and P. Vogel (Caltech) .

Observation of neutrinoless double-beta $(0\nu\beta\beta)$ decay would signal violation of total lepton number conservation. The process can be mediated by an exchange of a light Majorana neutrino, or by an exchange of other particles. However, the existence of $0\nu\beta\beta$ -decay requires a nonvanishing Majorana neutrino mass, no matter what the actual mechanism is. As long as only a limit on the lifetime is available, limits on the effective Majorana neutrino mass, on the lepton-number violating righthanded current or other possible mechanisms mediating $0\nu\beta\beta$ decay can be obtained, independently of the actual mechanism, by assuming that one of these "new physics" possibilities dominates. These limits are listed in the Double- β Decay Listings of the experimental measurements.

In the following we assume that the exchange of light Majorana neutrinos $(m_{\nu_i} \leq 10 \text{ MeV})$ contributes dominantly to the decay rate. Besides a dependence on the phase space $(G^{0\nu})$ and the nuclear matrix element $(M^{0\nu})$, the observable $0\nu\beta\beta$ -decay rate is proportional then to the square of the effective Majorana mass m_{ee} , $(T_{1/2}^{0\nu})^{-1} = G^{0\nu} \cdot |M^{0\nu}|^2 \cdot m_{ee}^2$, with $m_{ee}^2 = |\sum_i U_{ei}^2 m_{\nu_i}|^2$. The sum contains, in general, complex CP-phases in U_{ei}^2 , i.e., cancellations may occur. For three neutrino flavors there are two physical phases for Majorana neutrinos (η_1, η_2) and one for Dirac neutrinos (δ_{CP}) . The relevant Majorana phases affect only processes to which lepton-number changing amplitudes contribute. Given the general 3×3 mixing matrix for Majorana neutrinos, one can construct

https://pdg.lbl.gov

Created: 5/31/2023 09:12

other analogous lepton number violating quantities, $m_{\ell\ell'} = \sum_i U_{\ell i} U_{\ell' i} m_{\nu_i} (\ell \text{ or } \ell' \neq e)$. However, these are currently much less constrained than m_{ee} .

Nuclear structure calculations are needed to deduce m_{ee} from the decay rate. While $G^{0\nu}$ can be calculated accurately, the computation of $M^{0\nu}$ is subject to uncertainty. Comparing different nuclear model evaluations indicates a factor \sim 2-3 spread in the calculated nuclear matrix elements. Nuclear structure calculation consistently overestimate Gamow-Teller (axial current) matrix elements. This inability of the nuclear models to reproduce Gamow-Teller decay rates is often parametrized in form of a modified coupling constant q_A . Many nuclear theorists interpret this shortcoming as evidence that important physics is missing in the modeling of weak nuclear transitions. It is not clear how these observed uncertainties impact $0\nu\beta\beta$ -matrix elements. Nevertheless, this constitutes an additional element of uncertainty. Recent work, 1 shows how the discrepancy between experimental and theoretical axial current matrix elements might be resolved. However, application of this approach to the $0\nu\beta\beta$ decay remains to be accomplished. The particle physics quantities to be determined are thus nuclear model-dependent, so the half-life measurements are listed first. Where possible, we reference the nuclear matrix elements used in the subsequent analysis. Since rates for the conventional $2\nu\beta\beta$ decay serve to constrain the nuclear theory models, results for this process are also given.

Oscillation experiments utilizing atmospheric, accelerator, solar, and reactor produced neutrinos and anti-neutrinos show that at least some neutrinos are massive. However, so far the inverted mass ordering (i.e., whether $\Delta m_{31}^2 < 0$) is disfavored only by 2-3 σ compared to the normal mass ordering (when

 $\Delta m_{31}^2 > 0$), while the absolute neutrino mass values or the properties of neutrinos under CPT-conjugation (Dirac or Majorana) remain undetermined. All confirmed oscillation experiments can be consistently described using three interacting neutrino species with two mass splittings and three mixing angles. (For values of the mixing angles and mass square differences see the corresponding tables.)

Based on the 3-neutrino analysis:

 $e^{-2i(\eta_1+\delta_{CP})}\sin^2\theta_{13}m_3|^2$, valid for both mass orderings. Given the present knowledge of the neutrino oscillation parameters one can derive a relation between the effective Majorana mass and the mass of the lightest neutrino, as illustrated in Figure 14.11 in the Neutrino Masses, Mixing and Oscillations review. The three mass orderings allowed by the oscillation data: normal $(m_1 < m_2 \ll m_3)$, inverted $(m_3 \ll m_1 < m_2)$, and degenerate $(m_1 \approx m_2 \approx m_3)$, result in different projections. The width of the colored bands reflects the uncertainty introduced by the unknown Majorana and Dirac phases as well as the experimental errors of the oscillation parameters. The latter causes only minor broadening of the bands. Because of the overlap of the different mass scenarios, a measurement of m_{ee} would not reveal which mass ordering is applicable, provided the value of m_{ee} is in the overlapping range.

Analogous plots depict the relation of m_{ee} with the summed neutrino mass $m_{tot} = m_1 + m_2 + m_3$, constrained by observational cosmology, and m_{ee} as a function of the average mass $m_{\nu_e}^{eff} = [\Sigma |U_{ei}|^2 m_{\nu_i}^2]^{1/2}$ determined through the analysis of the electron energy distribution in low energy beta decays. (See Fig. 1 of [2].) The oscillation data thus allow to test whether observed values of m_{ee} and m_{tot} or $m_{\nu_e}^{eff}$ are consistent within

the 3 neutrino framework. The rather large intrinsic width of the $\beta\beta$ -decay constraints essentially does not allow to positively identify the mass ordering, and thus the sign of Δm_{31}^2 , even in combination with these other observables. Naturally, if a value of $0 < m_{ee} \leq 0.01$ eV is ever established, then the normal mass ordering becomes the only possible scenario.

It should be noted that systematic uncertainties of the nuclear matrix elements and possible quenching of the axial current matrix elements are sometimes not folded into the mass limits reported by $\beta\beta$ -decay experiments. Taking this additional uncertainty into account would further widen the projections. The plots are based on a 3-neutrino analysis. If it turns out that additional, i.e. sterile light neutrinos exist, the allowed regions would be modified substantially.

If neutrinoless double-beta decay is observed, it will be possible to fix a range of absolute values of the masses m_{ν_i} . Unlike the direct neutrino mass measurements, however, a limit on m_{ee} does not allow one to constrain the individual mass values m_{ν_i} even when the mass differences Δm_{ij}^2 are known.

Neutrino oscillation data imply the existence of a lower limit ~ 0.014 eV for the Majorana neutrino mass for the inverted mass ordering pattern, while m_{ee} could, by fine tuning, vanish in the case of the normal mass ordering. Several new doublebeta searches have been proposed to probe the interesting m_{ee} mass range, with the prospect of full coverage of the inverted mass ordering region within the next decade.

The $0\nu\beta\beta$ decay mechanism discussed so far is not the only way in which the decay can occur. Numerous other possible scenarios have been proposed, however, all of them requiring new physics. It will be a challenging task to decide which mechanism was responsible once $0\nu\beta\beta$ decay is observed. LHC experiments may reveal corresponding signatures for new

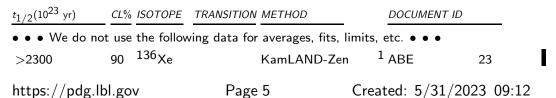
physics of lepton number violation. If lepton-number violating right-handed weak current interactions exist, its strength can be characterized by the phenomenological coupling constants η and λ (η describes the coupling between the right-handed lepton current and left-handed quark current while λ describes the coupling when both currents are right-handed). The $0\nu\beta\beta$ decay rate then depends on $\langle \eta \rangle = \eta \sum_{i} U_{ei} V_{ei}$ and $\langle \lambda \rangle = \lambda \sum_{i} U_{ei} V_{ei}$ that vanish for massless or unmixed neutrinos $(V_{\ell j})$ is a matrix analogous to $U_{\ell i}$ but describing the mixing with the hypothetical right-handed neutrinos). The observation of the single electron spectra could, in principle, allow to distinguish this mechanism of $0\nu\beta\beta$ from the light Majorana neutrino exchange driven mode. The limits on $\langle \eta \rangle$ and $\langle \lambda \rangle$ are listed in a separate table. The reader is cautioned that a number of earlier experiments did not distinguish between η and λ . In addition, see the section on Majoron searches for additional limits set by these experiments.

References

- P. Gysbers *et al.*, Nature Phys. **15**, 5 (2019); [arXiv:1903.00047].
- M.J. Dolinski, A.W.P. Poon and W. Rodejohann, Ann. Rev. Nucl. Part. Sci. 49, 219 (2019); [arXiv:1902.04097].

Half-life 0ν double- β decay

In most cases the transitions (Z,A) \rightarrow (Z+2,A) + 2e⁻ to the 0⁺ ground state of the final nucleus are listed. We also list transitions that decrease the nuclear charge (2e⁺, e⁺ CC and double EC) and transitions to an excited state of the final nucleus (0⁺_i, 2⁺, and 2⁺_i). In the following Listings only the best or comparable limits for the half-lives of each transition are reported and only those with about T_{1/2} > 10²³ years that are relevant for particle physics.



> 830 90 ⁷⁶ Ge MAJORANA ² ARNQUIST	23
$ > 830 \qquad 90 {}^{70}Ge \qquad MAJORANA \qquad {}^{2}ARNQUIST \\ > 220 \qquad 90 {}^{130}Te \qquad CUORE \qquad {}^{3}ADAMS $	23 22A
> 36 90 ¹²⁸ Te CUORE ⁴ ADAMS	22A 22B
> 12 90 ^{136}Xe XENON1T $^{5}APRILE$	22B 22A
> 18 90 100 Mo CUPID-Mo ⁶ AUGIER	22
> 46 90 ⁸² Se CUPID-0 ⁷ AZZOLINI	22
> 1.8 90 ⁸² Se g.s. $\rightarrow 0^+_1$ CUPID-0 ⁸ AZZOLINI	22
$> 3.0 \qquad 90^{-82} \text{Se} \text{g.s.} \rightarrow 2^+_1 \text{ CUPID-0} \qquad 9^{-9} \text{ AZZOLINI}$	22
$> 3.2 \qquad 90^{-82} \text{Se} \qquad \text{g.s.} \rightarrow 2^+_2 \text{ CUPID-0} \qquad ^{10} \text{ AZZOLINI}$	22
> 59 90 130 Te g.s. $\rightarrow 0^+_1$ CUORE 11 ADAMS	21A
> 15 90 ¹⁰⁰ Mo CUPID-Mo ¹² ARMENGAU	
> 39.9 90 76 Ge g.s. $\rightarrow 0^+_1$ MAJORANA-Dem 13 ARNQUIST	21
	21
> 21.2 90 ⁷⁰ Ge g.s. $\rightarrow 2_1^+$ MAJORANA-Dem ¹⁴ ARNQUIST > 9.7 90 ⁷⁶ Ge g.s. $\rightarrow 2_2^+$ MAJORANA-Dem ¹⁵ ARNQUIST	
- /	21
	20A
	20B
> 14 90 $\frac{130}{100}$ Te g.s. $\rightarrow 0^+_1$ CUORE-0 18 ALDUINO	19
> 0.95 90 100 Mo AMoRE 19 ALENKOV	19
> 350 90 136 Xe EXO-200 20 ANTON	19
> 2.4 90 ¹³⁶ Xe PANDAX-II ²¹ NI 130	19
> 150 90 ¹³⁰ Te CUORE ²² ALDUINO	18
> 2.5 90 ⁸² Se NEMO-3 ²³ ARNOLD	18
> 2.2 90 ¹¹⁶ Cd AURORA ²⁴ BARABASH ²⁵ \rightarrow 25 \rightarrow 26 \rightarrow 26 \rightarrow 26 \rightarrow 26 \rightarrow 26 \rightarrow 26 \rightarrow 26 \rightarrow 26 \rightarrow 26 \rightarrow 26 \rightarrow	18
> 1.1 90 ¹³⁴ Xe EXO-200 ²⁵ ALBERT	17C
$ \begin{array}{cccccccccccccccccccccccccccccccccccc$	17
	16
> 260 90 $\frac{136}{126}$ Xe g.s. $\rightarrow 2^+_1$ KamLAND-Zen $\frac{28}{128}$ ASAKURA	16
> 260 90 $\frac{136}{2}$ g.s. $\rightarrow 2^+_2$ KamLAND-Zen $\frac{29}{2}$ ASAKURA	16
> 240 90 136 Xe g.s. $\rightarrow 0^+_1$ KamLAND-Zen 30 ASAKURA	16
> 11 90 100 Mo NEMO-3 31 ARNOLD	15
$>$ 9.4 90 130 Te g.s. $ ightarrow$ 0 $^+_1$ CUORICINO 32 ANDREOTT	I 12
$> 0.58 ext{ 90} ext{ 48}$ Ca	08
$>$ 0.89 90 100 Mo g.s. \rightarrow 0 $^+_1$ NEMO-3 34 ARNOLD	07
$>$ 1.6 90 ¹⁰⁰ Mo g.s. $\rightarrow 2^{+}$ NEMO-3 ³⁵ ARNOLD	07
> 1.1 90 ¹²⁸ Te Cryog. det. ³⁶ ARNABOLD	I 03
> 1.7 90 ¹¹⁶ Cd ¹¹⁶ CdWO ₄ scint. ³⁷ DANEVICH	03
> 157 90 ⁷⁶ Ge Enriched HPGe ³⁸ AALSETH	0 2B

 $^1\,\text{ABE}$ 23 use the combined data set of the KamLAND-Zen 400 and 800 experiments, utilizing 745 kg of isotopically enriched xenon (90.9% ^{136}Xe), dissolved in liquid scintillator and an exposure of 970 kg·yr of ^{136}Xe , to derive this limit on $0\nu\beta\beta$ decay. A half-life sensitivity of 1.5×10^{26} yr is reported.

²ARNQUIST 23 use the final data set of the MAJORANA DEMONSTRATOR experiment, operating enriched in ⁷⁶Ge detectors, to set this limit on the $0\nu\beta\beta$ half-life of ⁷⁶Ge. The exposure is 64.5 kg·yr. A median sensitivity of 8.1×10^{25} yr is reported.

- ³ ADAMS 22A use the CUORE TeO₂ experiment with an exposure of 288.8 kg·yr of ¹³⁰Te to place a limit on its 0 ν $\beta\beta$ decay. The median sensitivity is reported as 280 × 10²³ yr. Superseeds ADAMS 20A.
- ⁴ ADAMS 22B use the CUORE bolometric calorimeter to place a limit on the $0\nu\beta\beta$ decay half-life of ¹²⁸ Te.
- 5 APRILE 22A use 36.16 kg·yr of $^{136}\rm Xe$ exposure of the XENON1T not enriched detector to establish the stated limit.
- ⁶ AUGIER 22 use the final data set of the CUPID-Mo cryogenic calorimeter, utilizing enriched $\text{Li}_2^{100}\text{MoO}_4$ and an isotope exposure of 1.47 kg·y, to place a limit on the $0\nu\beta\beta$ decay half-life.
- ⁷ AZZOLINI 22 use the CUPID-0 scintillating cryogenic bolometer to set a limit on the $0\nu\beta\beta$ half-life of ⁸²Se. The analyzed isotope exposure is 8.82 kg·yr. A median sensitivity of 7×10^{24} yr is reported. Supersedes AZZOLINI 19.
- ⁸AZZOLINI 22 use CUPID-0 data with an isotope exposure of 8.82 kg·yr to set a limit on the $0\nu\beta\beta$ decay to the first excited 0^+ state.
- ⁹AZZOLINI 22 use CUPID-0 data with an isotope exposure of 8.82 kg·yr to set a limit on the $0\nu\beta\beta$ decay to the first excited 2⁺ state.
- ¹⁰AZZOLINI 22 use CUPID-0 data with an isotope exposure of 8.82 kg·yr to set a limit on the $0\nu\beta\beta$ decay to the second excited 2⁺ state.
- ¹¹ ADAMS 21A et al. used 101.76 kg yr of ¹³⁰Te exposure of the CUORE (LNGS) bolometric detector to place a limit on the decay to the first excited state of ¹³⁰Xe, superseding ALDUINO 19 as the most restrictive bound on this particular decay.
- 12 ARMENGAUD 21 use the CUPID-Mo 4.2 kg array of enriched ${\rm Li_2}^{100}{\rm MoO_4}$ scintillating bolometers, with 1.17 kg·yr exposure, to set this limit.
- ¹³ ARNQUIST 21 use the MAJORANA demonstrator to set this limit for the 0 ν $\beta\beta$ decay to the first excited 0⁺ state, with a 41.9 kg yr isotopic exposure. The median sensitivity is 39.9 × 10²³ yr.
- ¹⁴ ARNQUIST 21 use the MAJORANA demonstrator to set this limit for the 0 ν $\beta\beta$ decay to the first excited 2⁺ state, with a 41.9 kg yr isotopic exposure. The median sensitivity is 21.2 × 10²³ yr.
- 15 ARNQUIST 21 use the MAJORANA demonstrator to set this limit for the 0 ν β β decay to the second excited 2⁺ state, with a 41.9 kg yr isotopic exposure. The median sensitivity is 18.6 \times 10²³ yr.
- 16 ADAMS 20A use the CUORE detector to search for the 0ν $\beta\beta$ decay of 130 Te. The exposure was 372.5 kg·yr of TeO_2 corresponding to 103.6 kg·yr of 130 Te. The exclusion sensitivity is 1.7×10^{25} yr. Supersedes ALDUINO 18.
- ¹⁷ AGOSTINI 20B present the final data set of the GERDA experiment, searching for $0\nu \beta\beta$ decay of ⁷⁶Ge with isotopically enriched, high resolution Ge detectors. A final exposure of 127.2 kg·yr is reported. The experiment reports the lowest background and longest half life limit ever achieved by any double beta decay experiment. The reported experiment sensitivity equals the limit. Supersedes AGOSTINI 19.
- ¹⁸ ALDUINO 19 use the combined data of the CUORICINO and CUORE-0 experiments to place a lower limit on the half life of the $0\nu \beta\beta$ decay of ¹³⁰Te to the first excited 0⁺ state of ¹³⁰Xe. Supersedes ANDREOTTI 12.
- $^{19}\,\text{ALENKOV}$ 19 report the 0ν $\beta\beta$ decay half-life limit based on the 52.1 kg d exposure of $^{100}\,\text{Mo}$, of a a cryogenic dual heat and light detector in the Yangyang underground laboratory. The median sensitivity is 1.1×10^{23} years.
- 20 ANTON 19 uses he complete dataset of the EXO-200 detector to search for the 0 ν $\beta\beta$ decay. The exposure is 234.1 kg yr. The median sensitivity is 5.0 \times 10 25 yr. Supersedes ALBERT 18 and ALBERT 14B.

- ²¹ NI 19 use the PandaX-II dual phase TPC at CJPL to search for the $0\nu \beta\beta$ decay of 136 Xe. The half-life limit 2.4 $\times 10^{23}$ yr is obtained from 22.2 kg yr exposure with a sensitivity of 1.9×10^{23} yr.
- ²² ALDUINO 18 uses the CUORE detector to search for the 0 ν $\beta\beta$ decay of ¹³⁰Te. The exposure is 86.3 kg·year of natural TeO₂ corresponding to 24.0 kg·year for ¹³⁰Te. The median sensitivity is 0.7 × 10²⁵ yr. The limit is obtained combining the new data from CUORE with those of CUOREO (9.8 kg·year of ¹³⁰Te) and Cuoricino (19.8 kg·year of ¹³⁰Te).
- 23 ARNOLD 18 use the NEMO-3 tracking detector to place a limit on the 0 $\nu\,\beta\,\beta$ decay of 82 Se. This is a slightly weaker limit than in BARABASH 11A, using the same detector. Supersedes ARNOLD 05A.
- 24 BARABASH 18 use 1.162 kg of 116 CdWO_4 scintillating crystals to obtain this limit. Supersedes DANEVICH 03 with analogous source and is more sensitive than ARNOLD 17.
- 25 ALBERT 17C uses the EXO-200 detector that contains 19.098 \pm 0.014% admixture of 134 Xe to search for the 0ν and 2ν $\beta\beta$ decay modes. The exposure is 29.6 kg·year. The median sensitivity is 1.9×10^{21} years.
- ²⁶ ARNOLD 17 use the NEMO-3 tracking calorimeter, containing 410 g of enriched ¹¹⁶Cd exposed for 5.26 yr, to determine the half-life limit. Supersedes BARABASH 11A.
- ²⁷ ALDUINO 16 report result obtained with 9.8 kg·y of data collected with the CUORE-0 bolometer, combined with data from the CUORICINO. Supersedes ALFONSO 15.
- 28 ASAKURA 16 use the KamLAND-Zen liquid scintillator calorimeter (136 Xe 89.5 kg yr) to place a limit on the $0\nu\beta\beta$ -decay into the first excited state of the daughter nuclide.
- ²⁹ASAKURA 16 use the KamLAND-Zen liquid scintillator calorimeter (¹³⁶Xe 89.5 kg yr) to place a limit on the $0\nu\beta\beta$ -decay into the second excited state of the daughter nuclide.
- ³⁰ASAKURA 16 use the KamLAND-Zen liquid scintillator calorimeter (¹³⁶Xe 89.5 kg yr) to place a limit on the $0\nu\beta\beta$ -decay into the third excited state of the daughter nuclide.
- ³¹ ARNOLD 15 use the NEMO-3 tracking calorimeter with 34.3 kg yr exposure to determine the limit of $0\nu\beta\beta$ -half life of ¹⁰⁰Mo. Supersedes ARNOLD 2005A and BARABASH 11A.
- 32 ANDREOTTI 12 use high resolution TeO₂ bolometric calorimeter to search for the $0\nu\beta\beta$ decay of 130 Te leading to the excited 0^1_+ state at 1793.5 keV.
- ³³ UMEHARA 08 use CaF₂ scintillation calorimeter to search for double beta decay of 48 Ca. Limit is significantly more stringent than quoted sensitivity: 18×10^{21} years.
- ³⁴Limit on 0ν -decay to the first excited 0^+_1 -state of daughter nucleus using NEMO-3 tracking calorimeter. Supersedes DASSIE 95.
- 35 Limit on 0ν -decay to the first excited 2⁺-state of daughter nucleus using NEMO-3 tracking calorimeter.
- ³⁶ Supersedes ALESSANDRELLO 00. Array of TeO₂ crystals in high resolution cryogenic calorimeter. Some enriched in ¹²⁸Te. Ground state to ground state decay.
- 37 Limit on $0\nu\beta\beta$ decay of 116 Cd using enriched CdWO_4 scintillators. Supersedes DANEVICH 00.
- ³⁸ AALSETH 02B limit is based on 117 mol·yr of data using enriched Ge detectors. Background reduction by means of pulse shape analysis is applied to part of the data set. Reported limit is slightly less restrictive than that in KLAPDOR-KLEINGROTHAUS 01 However, it excludes part of the allowed half-life range reported in KLAPDOR-KLEINGROTHAUS 01B for the same nuclide. The analysis has been criticized in KLAPDOR-KLEINGROTHAUS 04B. The criticism was addressed and disputed in AALSETH 04.

Half-life measurements of the two-neutrino double- β decay

The measured half-life values for the transitions $(Z,A) \rightarrow (Z+2,A) + 2e^- + 2\overline{\nu}_e$ to the 0⁺ ground state of the final nucleus are listed. We also list the transitions to an excited state of the final nucleus $(0_i^+, \text{ etc.})$. We report only the measuremetnts with the smallest (or comparable) uncertainty for each transition.

$t_{1/2}(10^{21} { m yr})$				SOTOPE	TRANSITIO	VMETHOD		DOCUMENT ID	
ullet $ullet$ $ullet$ We do not use the following data for averages, fits, limits, etc. $ullet$ $ullet$ $ullet$									
2190 11	±7 ±		± 1	¹²⁸ Те ¹²⁴ Хе		CUORE XENON1T		ADAMS APRILE	22в 22а
11.8		1.3	± 1.4	¹²⁴ Xe		XENONnT		APRILE	22B
2.34	+	0.08 0.46	$^{+0.30}_{-0.17}$	¹³⁶ Xe		NEXT	4	NOVELLA	22
0.771	—	0.008 0.006	$^{+0.012}_{-0.015}$	¹³⁰ Te		CUORE	5	ADAMS	21
0.00712	+	0.00018	± 0.00010	¹⁰⁰ Mo		CUPID-Mo	6	ARMENGAUD	20
18	±	5	± 1		$2\nu \text{DEC}$	XENON1T	7	APRILE	19E
0.00680	±	0.00001	+0.00038 -0.00040	¹⁰⁰ Mo		NEMO-3	8	ARNOLD	19
0.0860	±	0.0003	$^{+0.0019}_{-0.0013}$	⁸² Se		CUPID-0	9	AZZOLINI	19 B
0.0939	±	0.0017	± 0.0058	⁸² Se		NEMO-3	10	ARNOLD	18
0.0263	+	0.0011 0.0012		¹¹⁶ Cd		AURORA	11	BARABASH	18
> 0.87				¹³⁴ Xe		EXO-200		ALBERT	17 C
0.82	±	0.02	± 0.06	¹³⁰ Te		CUORE-0		ALDUINO	17
0.00690	±	0.00015	± 0.00037	¹⁰⁰ Mo		CUPID	14	ARMENGAUD	17
0.0274	±	0.0004	± 0.0018	^{116}Cd		NEMO-3	15	ARNOLD	17
0.064	—	0.007 0.006	$^{+0.012}_{-0.009}$	⁴⁸ Ca		NEMO-3	16	ARNOLD	16
0.00934	±	0.00022	$+0.00062 \\ -0.00060$	¹⁵⁰ Nd		NEMO-3		ARNOLD	16A
1.926	±	0.094		^{76}Ge		GERDA	18	AGOSTINI	15A
0.00693	±	0.00004	Ļ	¹⁰⁰ Mo		NEMO-3		ARNOLD	15
2.165	±	0.016	± 0.059	¹³⁶ Xe		EXO-200	20	ALBERT	14
9.2	+	5.5 2.6	± 1.3	⁷⁸ Kr		BAKSAN		GAVRILYAK	13
2.38	±	0.02	± 0.14	¹³⁶ Xe		KamLAND-Z			12A
0.7	±	0.09	± 0.11	¹³⁰ Te		NEMO-3		ARNOLD	11
0.0235	±	0.0014	± 0.0016	⁹⁶ Zr		NEMO-3	24	ARGYRIADES	10
0.69	+	0.10 0.08	± 0.07	¹⁰⁰ Mo	$0^+ \rightarrow 0^+_1$	Ge coinc.	25	BELLI	10
0.57	+	0.13 0.09	± 0.08		${\tt 0^+ \to 0^+_1}$	NEMO-3		ARNOLD	07
0.096	±	0.003	± 0.010	⁸² Se		NEMO-3	27	ARNOLD	05A
0.029	+	0.004 0.003		¹¹⁶ Cd		CdWO ₄ sc.	28	DANEVICH	03

 1 ADAMS 22B derive the $2\nu\,\beta\,\beta$ half-life of $^{128}{\rm Te}$ from data of the CUORE bolometric calorimeter and the half-live ratio for $^{130}{\rm Te}$ / $^{128}{\rm Te}$ reported in BERNATOWICZ 92.

- 2 APRILE 22A report an improved 124 Xe $_{2\nu}$ DEC half-life measurement for 124 Xe, using data collected by the XENON1T detector with an isotopically not enriched Xe target. The analyzed 124 Xe exposure is 0.87 kg·yr. The statistical significance of the signal is 7.0 sigma. The stated half-life considers captures from the K shell up to the N5 shell. This result supersedes APRILE 19E, which exclusively considered captures from the K shell.
- ³APRILE 22B use data collected by the XENONnT dark matter experiment to derive an improved ¹²⁴Xe 2ν DEC half-life measurement for ¹²⁴Xe. This result supersedes APRILE 22A.
- ⁴ NOVELLA 22 report on a high-pressure gas TPC at Canfranc underground laboratory, filled with 3.5 kg (fiducial) xenon gas, used to measure the $2\nu \beta\beta$ decay of ¹³⁶Xe. Topological track reconstruction is utilized in the data analysis. The measurement is based on comparing runs with isotopically enriched and depleted xenon. Other measurements with smaller error exist.
- ⁵ ADAMS 21 use 102.7 kg yr of ¹³⁰Te exposure, collected by the CUORE bolometric detector at LNGS, to perform the most precise measurement of $2\nu \beta\beta$ decay of this nuclide to date. The dataset is more than 10-times that used by the CUORE-0 experiment. Supersedes ALDUINO 17.
- ⁶ ARMENGAUD 20 use the Li₂¹⁰⁰MoO₄ scintillating bolometers to determine the halflife of the $2\nu \beta\beta$ decay of ¹⁰⁰Mo. The total exposure was 42.235 kg·d. The single-state dominance for this decay is favored at > 3 σ .
- 7 APRILE 19E report first measurement of two-neutrino double electron capture in $^{124}{\rm Xe}$ using the XENON1T detector with a 0.73 t-yr exposure. An excess of 126 \pm 29 events

is observed at 64.3 \pm 0.6 keV decay energy, corresponding to $\sqrt{\Delta\chi^2}$ = 4.4 with respect to the background-only hypothesis.

- ⁸ ARNOLD 19 use the NEMO-3 tracking calorimeter with 34.3 kg y exposure to determine the $2\nu \beta\beta$ half-life of ¹⁰⁰Mo. Supersedes ARNOLD 15.
- ⁹AZZOLINI 19B use the CUPID-0 experiment, utilizing ZnSe bolometers and an exposure of 9.95 kg yr of Zn⁸²Se, to determine the half-life of the $2\nu \beta\beta$ decay of ⁸²Se. The analysis provides evidence for single state dominance showing that the higher state dominance is disfavored at the level of 5.5 σ .
- ¹⁰ ARNOLD 18 use the NEMO-3 tracking detector to determine the $2\nu\beta\beta$ half-life of ⁸²Se. 0.93 kg of ⁸²Se was observed for 5.25 y. The half-life value was obtained based on the single-state-dominance (SSD) hypothesis, preferred in this case by about 2 σ . Supersedes ARNOLD 05A.
- 11 BARABASH 18 use 1.162 kg of 116 CdWO_4 scintillating crystals to obtain this value. Supersedes DANEVICH 03 with analogous source and agrees with ARNOLD 17 with the NEMO-3 detector.
- 12 ALBERT 17C uses the EXO-200 detector that contains 19.098 \pm 0.014% admixture of 134 Xe to search for the 2ν $\beta\beta$ decay mode. The exposure is 29.6 kg·year. The median sensitivity is 1.2×10^{21} years.
- ¹³ ALDUINO 17 use the CUORE-0 detector containing 10.8 kg of 130 Te in 52 crystals of TeO₂. The exposure was 9.3 kg yr of 130 Te. This is a more accurate rate determination than in ARNOLD 11 and BARABASH 11A.
- ¹⁴ ARMENGAUD 17 use 185.9 \pm 0.1 g crystal of Li₂¹⁰⁰MoO₄ to determine the ¹⁰⁰Mo $2\nu \beta\beta$ half-life. The exposure was of 1303 \pm 26 hours only, using novel technique.
- ¹⁵ ARNOLD 17 use the NEMO-3 tracking calorimeter, containing 410 grams of enriched ¹¹⁶Cd exposed for 5.26 years, to determine the half-life value.
- ¹⁶ ARNOLD 16 use the NEMO-3 detector and a source of 6.99 g of ⁴⁸Ca. The half-life is based on 36.7 g year exposure. It is consistent, although somewhat longer, than the previous determinations of the half-life. Supersedes BARABASH 11A.
- 17 ARNOLD 16A use the NEMO-3 tracking calorimeter, containing 36.6 g of 150 Nd exposed for 1918.5 days, to determine the half-life. Supersedes ARGYRIADES 09.
- ¹⁸ AGOSTINI 15A use 17.9 kg yr exposure of the GERDA calorimeter to derive an improved measurement of the $2\nu\beta\beta$ decay half life of ⁷⁶Ge.

- 19 ARNOLD 15 use the NEMO-3 tracking calorimeter with 34.3 kg yr exposure to determine the $2\nu\beta\beta$ -half life of ¹⁰⁰Mo. Supersedes ARNOLD 05A and ARNOLD 04.
- ²⁰ ALBERT 14 use the EXO-200 tracking detector for a re-measurement of the $2\nu\beta\beta$ -half life of ¹³⁶Xe. A nuclear matrix element of $0.0218 \pm 0.0003 \text{ MeV}^{-1}$ is derived from this data. Supersedes ACKERMAN 11.
- 21 GAVRILYAK 13 use a proportional counter filled with Kr gas to search for the 2
 u2K decay of ⁷⁸Kr. Data with the enriched and depleted Kr were used to determine signal and background. A 2.5 σ excess of events obtained with the enriched sample is interpreted as an indication for the presence of this decay.
- 22 GANDO 12A use a modification of the existing KamLAND detector. The etaeta decay source/detector is 13 tons of enriched ¹³⁶Xe-loaded scintillator contained in an inner balloon. The $2\nu\beta\beta$ decay rate is derived from the fit to the spectrum between 0.5 and 4.8 MeV. This result is in agreement with ACKERMAN 11.
- ²³ ARNOLD 11 use enriched ¹³⁰Te in the NEMO-3 detector to measure the $2\nu \beta\beta$ decay rate. This result is in agreement with, but more accurate than ARNABOLDI 03. ²⁴ ARGYRIADES 10 use 9.4 ± 0.2 g of ⁹⁶Zr in NEMO-3 detector and identify its $2\nu\beta\beta$ decay. The result is in agreement and supersedes ARNOLD 99.
- ²⁵ BELLI 10 use enriched ¹⁰⁰Mo with 4 HP Ge detectors to record the 590.8 and 539.5 keV γ rays from the decay of the 0⁺₁ state in ¹⁰⁰Ru both in singles and coincidences. This result confirms the measurement of KIDD 09 and ARNOLD 07 and supersedes them.
- ²⁶ First exclusive measurement of 2ν -decay to the first excited 0^+_1 -state of daughter nucleus. ARNOLD 07 use the NEMO-3 tracking calorimeter to detect all particles emitted in decay. Result agrees with the inclusive $(0\nu + 2\nu)$ measurement of DEBRAECKELEER 01.
- 27 ARNOLD 05A use the NEMO-3 tracking detector to determine the 2
 uetaetaeta half-life of ⁸²Se with high statistics and low background (389 days of data taking). Supersedes ARNOLD 04.
- ²⁸ DANEVICH 03 is calorimetric measurement of $2\nu\beta\beta$ ground state decay of ¹¹⁶Cd using enrichedCdWO₄ scintillators. Agrees with EJIRI 95 and ARNOLD 96. Supersedes DANEVICH 00.

$\langle m_{ee} \rangle$, The Effective Weighted Sum of Majorana Neutrino Masses Contributing to Neutrinoless Double- β Decay

 $\langle m_{\rm ee} \rangle = |\Sigma U_{ei}^2 m_{\nu_i}|$, i = 1,2,3. It is assumed that ν_i are Majorana particles and that the transition is dominated by the known (light) neutrinos. Note that U_{ei}^2 and not $|U_{ei}|^2$ occur in the sum, and that consequently cancellations are possible. The experiments obtain the limits on $\langle m_{
u}
angle$ from the measured ones on $T_{1/2}$ using a range of nuclear matrix elements (NME), which is reflected in the spread of $\langle m_{
u}
angle$. Different experiments may choose different NME. All assume $g_A = 1.27$. In the following Listings, only the best or comparable limits for each isotope are reported. When not mentioned explicitly the transition is between ground states, but transitions between excited states are also reported.

VALUE (eV)	ISOTOPE	METHOD	DOCUMENT ID	
$\bullet \bullet \bullet$ We do not use the	e following	data for averages, fits,	limits, etc. • • •	
< 0.036-0.156	136 Xe	KamLAND-Zen	¹ ABE	23
< 0.113-0.269	⁷⁶ Ge	MAJORANA	² ARNQUIST	23
< 0.09–0.305	¹³⁰ Te	CUORE	³ ADAMS	22A
< 0.8–2.5	¹³⁶ Xe	XENON1T	⁴ APRILE	22A
< 0.28–0.49	100 _{Mo}	CUPID-Mo	⁵ AUGIER	22

$ \begin{array}{c ccccccccccccccccccccccccccccccccccc$	< 1.6–5.3 < 0.33–0.62 < 7.2–19.5 < 3.5–22	150 _{Nd} 100 _{Mo} 96 _{Zr} 48 _{Ca}	NEMO-3 NEMO-3 NEMO-3 CaF ₂ scint.	 ¹⁸ ARNOLD ¹⁹ ARNOLD ²⁰ ARGYRIADES ²¹ UMEHARA 	20A 20B 19 19 18 18 18 18 17 16 16A 15 10 08
--	--	--	---	---	---

¹ABE 23 utilize 745 kg of 136 Xe isotope exposure from the combined data set of the KamLAND-Zen 400 and 800 to derive a limit on $\langle m_{\beta\beta} \rangle$. The range reflects the author's assessment of the variability of the theoretically calculated nuclear matrix elements.

- 2 ARNQUIST 23 use the final data set of the MAJORANA DEMONSTRATOR experiment, with 64.5 kg·yr of isotop exposure, to derive an upper limit for $\langle m_{\beta\beta} \rangle$. The range reflects the author's assessment of the variability of the theoretically calculated nuclear matrix elements.
- ³ADAMS 22A use 1038.4 kg yr of TeO₂ exposure collected by the CUORE experiment to determine this range of limits. The range reflects the uncertainty of nuclear matrix element calculations needed for the conversion of half-life to neutrino mass.
- ⁴ APRILE 22A use data taken with the XENON1T detector to limit the Majorana neutrino mass. 36.16 kg·yr of 136 Xe exposure were utilized. The reported range of limits is due to uncertainties in the nuclear matrix elements.
- 5 AUGIER 22 use the final data set of the CUPID-Mo cryogenic calorimeter with an isotop exposure of 1.47 kg·y to derive a range of neutrino mass limits. The range reflects the authors' estimate of the spread of nuclear matrix element calculations.
- ⁶AZZOLINI 22 use 8.82 kg·yr of isotopic exposure of the CPID-0 scintillating cryogenic bolometer to set this range of neutrino mass limits. The range reflects the authors' estimate of the spread of nuclear matrix element calculations.
- ⁷ ARMENGAUD 21 use the CUPID-Mo demonstrator, with 1.17 kg·yr exposure of 100 Mo, to set this limit. The range reflects the estimated uncertainty of the calculated nuclear matrix elements. 8 ADAMS 20A use the data of CUORE (372.5 kg·yr exposure of TeO₂) to obtain this limit.
- 9 AGOSTINI 20B use the final data set of the GERDA experiment, representing an exposure of 127.2 kg·yr to derive an upper limit for $\langle m_{\beta\beta} \rangle$. Isotopically enriched Ge detectors were used. The range reflects the variability of the theoretically calculated nuclear matrix elements. Supersedes AGOSTINI 19.
- 10 ALENKOV 19 report the range of the effective masses $\langle m_{eta\,eta}
 angle$ corresponding to the 0u $\beta\beta$ decay half-life limit. It is based on the 52.1 kg d exposure of 100 Mo, in the Yangyang underground laboratory. The median sensitivity is 1.1×10^{23} years. The range of $\langle m_{\beta\beta} \rangle$ reflects the uncertainty of nuclear matrix elements.
- 11 ANTON 19 uses the complete dataset of the EXO-200 experiment to obtain these limits. The spread reflect the uncertainty in the nuclear matrix elements. Supersedes ALBERT 18 and ALBERT 14B.

¹² NI 19 use the PandaX-II dual phase TPC at CJPL to search for the $0\nu \beta\beta$ decay of ¹³⁶Xe with 22.2 kg yr exposure. The range in the $m_{\beta\beta}$ limit of 1.3–3.5 eV reflects the

range of the calculated nuclear matrix elements. The sensitivity is 1.9×10^{23} yr.

- ¹³ ALDUINO 18 use the combined data of CUORE, CUORE0, and Cuoricino to obtain this limit.
- ¹⁴ ARNOLD 18 use the NEMO-3 tracking detector to constrain the $0\nu\beta\beta$ decay of ⁸²Se. The limit on $\langle m_{\beta\beta} \rangle$ is obtained assuming light neutrino exchange; the range reflects different calculations of the nuclear matrix elements. This is a somewhat weaker limit than in BARABASH 11A using the same detector.
- ¹⁵ BARABASH 18 use 1.162 kg of ¹¹⁶CdWO₄ scintillating crystals to obtain these limits. The spread reflects the estimated uncertainty in the nuclear matrix element. Supersedes DANEVICH 03.
- ¹⁶ ARNOLD 17 utilize NEMO-3 data, taken with enriched ¹¹⁶Cd to limit the effective Majorana neutrino mass. The reported range results from the use of different nuclear matrix elements. Supersedes BARABASH 11A.
- ¹⁷ ALDUINO 16 place a limit on the effective Majorana neutrino mass using the combined data of the CUORE-0 and CUORICINO experiments. The range reflects the authors' evaluation of the variability of the nuclear matrix elements. Supersededs ALFONSO 15.
- ¹⁸ ARNOLD 16A limit is derived from data taken with the NEMO-3 detector and ¹⁵⁰Nd. A range of nuclear matrix elements that include the effect of nuclear deformation have been used. Supersedes ARGYRIADES 09.
- ¹⁹ ARNOLD 15 use the NEMO-3 tracking calorimeter with 34.3 kg yr exposure to determine the neutrino mass limit based on the $0\nu\beta\beta$ -half life of ¹⁰⁰Mo. The spread range reflects different nuclear matrix elements. Supersedes ARNOLD 14 and BARABASH 11A.
- 20 ARGYRIADES 10 use $^{96}{\rm Zr}$ and the NEMO-3 tracking detector to obtain the reported mass limit. The range reflects the fluctuation of the nuclear matrix elements considered.
- 21 Limit was obtained using CaF $_2$ scintillation calorimeter to search for double beta decay of 48 Ca. Reported range of limits reflects spread of QRPA and SM matrix element calculations used. Supersedes OGAWA 04.
- 22 Limit for $\langle m_{\nu}\rangle$ is based on the nuclear matrix elements of STAUDT 90 and ARNOLD 96. Supersedes DANEVICH 00.

Limits on Lepton-Number Violating (V+A) Current Admixture

For reasons given in the discussion at the beginning of this section, we list only results from 1989 and later. $\langle \lambda \rangle = \lambda \sum U_{ej} V_{ej}$ and $\langle \eta \rangle = \eta \sum U_{ej} V_{ej}$, where the sum is over the number of neutrino generations. This sum vanishes for massless or unmixed neutrinos. In the following Listings, only best or comparable limits or lifetimes for each isotope are reported.

$\left<\lambda\right>$ (10 ⁻⁶)	CL%	$\left<\eta\right>$ (10 ⁻⁸)	CL%	ISOTOPE	METHOD	DOCUMENT ID	
• • • We de	o not	use the follov	ving d	ata for avei	rages, fits, limits, e	etc. • • •	
< 2.2–2.6	90	< 1.7–2.1	90	⁸² Se	NEMO-3	¹ ARNOLD	18
< 1.8–22	90	< 1.6–21	90	^{116}Cd	AURORA	² BARABASH	18
< 0.9–1.3	90	< 0.5–0.8	90	100 _{Mo}	NEMO-3	³ ARNOLD	14
<120	90			100 _{Mo}	$0^+ \rightarrow 2^+$	⁴ ARNOLD	07
$0.692 \substack{+0.05 \\ -0.05}$	8 6 ⁶⁸	$0.305 \substack{+0.02 \\ -0.02}$	6 5 68	76 _{Ge}	Enriched HPGe	⁵ KLAPDOR-K	. 06A
< 2.5	90		-	¹⁰⁰ Mo	0ν , NEMO-3	⁶ ARNOLD	05A
< 3.8	90			⁸² Se	0ν , NEMO-3	⁷ ARNOLD	05A
< 1.5 - 2.0	90			100 _{Mo}	0ν , NEMO-3	⁸ ARNOLD	04
< 3.2–3.8	90			⁸² Se	0ν , NEMO-3	⁹ ARNOLD	04
< 1.6-2.4	90	< 0.9–5.3	90	¹³⁰ Te	Cryog. det.	¹⁰ ARNABOLDI	03

< 2.2	90	<2.5	90	^{116}Cd	116 CdWO $_4$ scint	¹¹ DANEVICH	03
< 3.2–4.7	90	< 2.4–2.7	90	¹⁰⁰ Mo	ELEGANT V	-	01
< 1.1	90	<0.64		76_{Ge}	Enriched HPGe	¹³ GUENTHER	
< 4.4	90	<2.3		¹³⁶ Xe	ТРС	¹⁴ VUILLEUMIEF	R 93
		<5.3		¹²⁸ Te	Geochem	¹⁵ BERNATOW	. 92

¹ARNOLD 18 use the NEMO03 tracking detector, with 0.93 kg of ⁸²Se mass and 5.25 y exposure to obtain the limits for the hypothetical right-handed currents. Supersedes ARNOLD 05A.

- ² BARABASH 18 use 1.162 kg of ¹¹⁶CdWO₄ scintillating crystals to obtain this limits for the hypothetical right-handed currents in the $0\nu\beta\beta$ decay of ¹¹⁶Cd.
- ³ARNOLD 14 is based on 34.7 kg yr of exposure of the NEMO-3 tracking calorimeter. The reported range limit on $\langle \lambda \rangle$ and $\langle \eta \rangle$ reflects the nuclear matrix element uncertainty in ¹⁰⁰Mo.
- ¹ ARNOLD 07 use NEMO-3 half life limit for 0ν -decay of ¹⁰⁰Mo to the first excited 2⁺state of daughter nucleus to limit the right-right handed admixture of weak currents $\langle \lambda \rangle$. This limit is not competitive when compared to the decay to the ground state.

⁵ Re-analysis of data originally published in KLAPDOR-KLEINGROTHAUS 04A. Modified pulse shape analysis leads the authors to claim 6σ statistical evidence for observation of 0ν -decay. Authors use matrix element of MUTO 89 to determine $\langle \lambda \rangle$ and $\langle \eta \rangle$. Uncertainty of nuclear matrix element is not reflected in stated errors.

⁶ ARNOLD 05A derive limit for $\langle \lambda \rangle$ based on ¹⁰⁰Mo data collected with NEMO-3 detector. No limit for $\langle \eta \rangle$ is given. Supersedes ARNOLD 04.

- ⁷ ARNOLD 05A derive limit for $\langle \lambda \rangle$ based on ⁸²Se data collected with NEMO-3 detector. No limit for $\langle \eta \rangle$ is given. Supersedes ARNOLD 04.
- ⁸ ARNOLD 04 use the matrix elements of SUHONEN 94 to obtain a limit for $\langle \lambda \rangle$, no limit for $\langle \eta \rangle$ is given. This limit is more stringent than the limit in EJIRI 01 for the same nucleus. ⁹ ARNOLD 04 use the matrix elements of TOMODA 91 and SUHONEN 91 to obtain a
- ⁹ARNOLD 04 use the matrix elements of TOMODA 91 and SUHONEN 91 to obtain a limit for $\langle \lambda \rangle$, no limit for $\langle \eta \rangle$ is given.
- ¹⁰ Supersedes ALESSANDRELLO 00. Cryogenic calorimeter search. Reported a range reflecting uncertainty in nuclear matrix element calculations.
- ¹¹ Limits for $\langle \lambda \rangle$ and $\langle \eta \rangle$ are based on nuclear matrix elements of STAUDT 90. Supersedes DANEVICH 00.
- ¹² The range of the reported $\langle \lambda \rangle$ and $\langle \eta \rangle$ values reflects the spread of the nuclear matrix elements. On axis value assuming $\langle m_{\mu} \rangle = 0$ and $\langle \lambda \rangle = \langle \eta \rangle = 0$, respectively.
- 13 GUENTHER 97 limits use the matrix elements of STAUDT 90. Supersedes BALYSH 95 , and BALYSH 92.
- 14 VUILLEUMIER 93 uses the matrix elements of MUTO 89. Based on a half-life limit 2.6×10^{23} y at 90%CL.
- ¹⁵ BERNATOWICZ 92 takes the measured geochemical decay width as a limit on the 0ν width, and uses the SUHONEN 91 coefficients to obtain the least restrictive limit on η . Further details of the experiment are given in BERNATOWICZ 93.

Double- β Decay REFERENCES

ABE ARNQUIST ADAMS ADAMS APRILE APRILE AUGIER AZZOLINI NOVELLA ADAMS ADAMS	23 23 22A 22B 22A 22B 22 22 22 22 21 21A	PRL 130 051801 PRL 130 062501 NAT 604 53 PRL 129 222501 PR C106 024328 PRL 129 161805 EPJ C82 1033 PRL 129 111801 PR C105 055501 PRL 126 171801 EPJ C81 567	 S. Abe et al. I.J. Arnquist et al. D.Q. Adams et al. D.Q. Adams et al. E. Aprile et al. E. Aprile et al. C. Augier et al. O. Azzolini et al. P. Novella et al. D.Q. Adams et al. D.Q. Adams et al. 	(KamLAND-Zen Collab.) (MAJORANA Collab.) (CUORE Collab.) (CUORE Collab.) (XENON1T Collab.) (XENONNT Collab.) (CUPID-Mo Collab.) (CUPID-0 Collab.) (NEXT Collab.) (CUORE Collab.)
ADAMS	21A	EPJ C81 567	D.Q. Adams <i>et al.</i>	(CUORE Collab.)

https://pdg.lbl.gov

Created: 5/31/2023 09:12

ARMENGAUD	21	PRL 126 181802	E. Armengaud <i>et al.</i>	(CUPID-Mo Collab.)
ARNQUIST	21	PR C103 015501	I.J. Arnquist <i>et al.</i>	(MAJORANA Collab.)
• .	20A			
ADAMS		PRL 124 122501	D.Q. Adams <i>et al.</i>	(CUORE Collab.)
AGOSTINI	20B	PRL 125 252502	M. Agostini <i>et al.</i>	(GERDA Collab.)
ARMENGAUD		EPJ C80 674	E. Armengaud <i>et al.</i>	(CUPID-Mo Collab.)
AGOSTINI	19	SCI 365 1445	M. Agostini <i>et al.</i>	(GERDA Collab.)
ALDUINO	19	EPJ C79 795	C. Alduino <i>et al.</i>	(CUORE Collab.)
ALENKOV	19	EPJ C79 791	V. Alenkov <i>et al.</i>	(AMoRE Collab.)
ANTON	19	PRL 123 161802	G. Anton <i>et al.</i>	(ÈXO-200 Collab.)
APRILE	19E	NAT 568 532	E. Aprile <i>et al.</i>	(XENON1T Collab.)
ARNOLD	19	EPJ C79 440	R. Arnold <i>et al.</i>	(NEMO-3 Collab.)
AZZOLINI	19	PRL 123 032501	O. Azzolini <i>et al.</i>	(CUPID-0 Collab.)
AZZOLINI	19B	PRL 123 262501	O. Azzolini <i>et al.</i>	(CUPID-0 Collab.)
NI	190	CP C43 113001	K. Ni et al.	(PandaX-II Collab.)
	-			(
ALBERT	18	PRL 120 072701	J.B. Albert <i>et al.</i>	(EXO-200 Collab.)
ALDUINO	18	PRL 120 132501	C. Alduino <i>et al.</i>	(CUORE Collab.)
ARNOLD	18	EPJ C78 821	R. Arnold <i>et al.</i>	(NEMO-3 Collab.)
BARABASH	18	PR D98 092007	A.S. Barabash <i>et al.</i>	(AURORA Collab.)
ALBERT	17C	PR D96 092001	J.B. Albert <i>et al.</i>	(EXO-200 Collab.)
ALDUINO	17	EPJ C77 13	C. Alduino <i>et al.</i>	(CUORE Collab.)
ARMENGAUD	17	EPJ C77 785	E. Armengaud <i>et al.</i>	(CUPID Collab.)
ARNOLD	17	PR D95 012007	R. Arnold <i>et al.</i>	(NEMO-3 Collab.)
ALDUINO	16	PR C93 045503	C. Alduino <i>et al.</i>	(CUORE Collab.)
ARNOLD	16	PR D93 112008	R. Arnold <i>et al.</i>	(NEMO-3 Collab.)
ARNOLD	16A	PR D94 072003	R. Arnold <i>et al.</i>	(NEMO-3 Collab.)
ASAKURA	16	NP A946 171	K. Asakura <i>et al.</i>	(KamLAND-Zen Collab.)
AGOSTINI	15A	EPJ C75 416	M. Agostini <i>et al.</i>	(GERDA Collab.)
				()
ALFONSO	15	PRL 115 102502	K. Alfonso <i>et al.</i>	(CUORE Collab.)
ARNOLD	15	PR D92 072011	R. Arnold <i>et al.</i>	(NEMO-3 Collab.)
ALBERT	14	PR C89 015502	J. Albert <i>et al.</i>	(EXO-200 Collab.)
ALBERT	14B	NAT 510 229	J.B. Albert <i>et al.</i>	(EXO-200 Collab.)
ARNOLD	14	PR D89 111101	R. Arnold <i>et al.</i>	(NEMO-3 Collab.)
GAVRILYAK	13	PR C87 035501	Yu.M. Gavrilyuk <i>et al.</i>	
ANDREOTTI	12	PR C85 045503	E. Andreotti <i>et al.</i>	(CUORICINO Collab.)
GANDO	12A	PR C85 045504	A. Gando <i>et al.</i>	(KamLAND-Zen Collab.)
ACKERMAN	11	PRL 107 212501	N. Ackerman <i>et al.</i>	(EXO Collab.)
ARNOLD	11	PRL 107 062504	R. Arnold <i>et al.</i>	(NEMO-3 Collab.)
BARABASH	11A	PAN 74 312	A.S. Barabash <i>et al.</i>	(NEMO-3 Collab.)
		Translated from YAF 74		
ARGYRIADES	10	NP A847 168	J. Argyriades <i>et al.</i>	(NEMO-3 Collab.)
BELLI	10	NP A846 143	P. Belli <i>et al.</i>	(DAMA-INR Collab.)
ARGYRIADES	09	PR C80 032501	J. Argyriades <i>et al.</i>	(NEMO-3 Collab.)
KIDD	09	NP A821 251	M. Kidd <i>et al.</i>	
UMEHARA	08	PR C78 058501	S. Umehara <i>et al.</i>	
ARNOLD	07	NP A781 209	R. Arnold <i>et al.</i>	(NEMO-3 Collab.)
KLAPDOR-K	06A	MPL A21 1547	H.V. Klapdor-Kleingrothaus,	I.V. Krivosheina
ARNOLD	05A	PRL 95 182302	R. Arnold <i>et al.</i>	(NEMO-3 Collab.)
AALSETH	04	PR D70 078302	C.E. Aalseth <i>et al.</i>	(
ARNOLD	04	JETPL 80 377	R. Arnold <i>et al.</i>	(NEMO-3 Collab.)
	•	Translated from ZETFP	80 429.	(
KLAPDOR-K	04A	PL B586 198	H.V. Klapdor-Kleingrothaus	et al.
KLAPDOR-K	04B	PR D70 078301	H.V. Klapdor-Kleingrothaus,	A. Dietz, I.V. Krivosheina
OGAWA	04	NP A730 215	I. Ogawa <i>et al.</i>	
ARNABOLDI	03	PL B557 167	C. Arnaboldi <i>et al.</i>	
DANEVICH	03	PR C68 035501	F.A. Danevich <i>et al.</i>	
AALSETH	02B	PR D65 092007	C.E. Aalseth <i>et al.</i>	(IGEX Collab.)
DEBRAECKEL.		PRL 86 3510	L. De Braeckeleer <i>et al.</i>	
EJIRI	01	PR C63 065501	H. Ejiri <i>et al.</i>	
KLAPDOR-K				at al
		EPJ A12 147	H.V. Klapdor-Kleingrothaus	
KLAPDOR-K		MPL A16 2409	H.V. Klapdor-Kleingrothaus	et al.
ALESSAND	00	PL B486 13	A. Alessandrello <i>et al.</i>	
DANEVICH	00	PR C62 045501	F.A. Danevich <i>et al.</i>	
ARNOLD	99	NP A658 299	R. Arnold <i>et al.</i>	(NEMO Collab.)
GUENTHER	97	PR D55 54	M. Gunther <i>et al.</i>	(Heidelberg-Moscow Collab.)
ARNOLD	96	ZPHY C72 239	R. Arnold <i>et al.</i>	(BCEN, CAEN, JINR+)
BALYSH	95	PL B356 450	A. Balysh <i>et al.</i>	(Heidelberg-Moscow Collab.)
DASSIE	95	PR D51 2090	D. Dassie <i>et al.</i>	(NEMO Collab.)
EJIRI	95	JPSJ 64 339	H. Ejiri <i>et al.</i>	(OSAK, KIEV)
SUHONEN	94	PR C49 3055	J. Suhonen, O. Civitarese	
BERNATOW	93	PR C47 806	T. Bernatowicz <i>et al.</i>	(WUSL, TATA)
VUILLEUMIER		PR C47 806 PR D48 1009	T. Bernatowicz <i>et al.</i> J.C. Vuilleumier <i>et al.</i>	(WUSL, TATA) (NEUC, CIT, VILL)

https://pdg.lbl.gov

Created: 5/31/2023 09:12

BALYSH 92	PL B283 32	A. Balysh <i>et al.</i> (MPIK, KIAE, SASSO)
BERNATOW 92	PRL 69 2341	T. Bernatowicz <i>et al.</i> (WUSL, TATA)
SUHONEN 91	NP A535 509	J. Suhonen, S.B. Khadkikar, A. Faessler (JYV+)
TOMODA 91	RPP 54 53	T. Tomoda
STAUDT 90	EPL 13 31	A. Staudt, K. Muto, H.V. Klapdor-Kleingrothaus
MUTO 89	ZPHY A334 187	K. Muto, E. Bender, H.V. Klapdor (TINT, MPIK)

Citation: R.L. Workman et al. (Particle Data Group), Prog. Theor. Exp. Phys. 2022, 083C01 (2022) and 2023 update